LIMNOLOGY
and
OCEANOGRAPHY

ASLO

Limnol. Oceanogr. 00, 2015, 1–25

doi: 10.1002/lno.10103

Stream oxygen flux and metabolism determined with the open water and aquatic eddy covariance techniques

Dirk J. Koopmans*[1,2] Peter Berg[1]
[1]Department of Environmental Sciences, University of Virginia, Charlottesville, Virginia
[2]School of Freshwater Sciences, University of Wisconsin-Milwaukee, Milwaukee, Wisconsin

Abstract

We quantified oxygen flux in a coastal stream in Virginia using a novel combination of the conventional open water technique and the aquatic eddy covariance technique. The latter has a smaller footprint (sediment surface area that contributes to the flux; $\sim 10\,m^2$), allowing measurements to be made at multiple sites within the footprint of the open water technique ($\sim 1000\,m^2$). Sites included an unvegetated stream pool with cohesive sediment, a macrophyte bed with sandy sediment, and an unvegetated sand bed with rippled bedforms. Nighttime eddy covariance oxygen uptake was always smaller than uptake produced by the open water technique. At the pool and unvegetated sand bed sites, nighttime eddy covariance uptake was 20-fold smaller than open water uptake. At the macrophyte bed site, gross primary production quantified with the two techniques was similar but eddy covariance uptake was 2.4-fold smaller. The difference in oxygen uptake between eddy covariance and open water techniques could not be accounted for by uncertainties in the gas transfer velocity but could be accounted for by anoxic groundwater inflow through stream banks outside of the eddy covariance footprint. Nighttime oxygen uptake was also measured with eddy covariance in a tidal freshwater part of the stream, where pore space in the sandy sediment near the sediment–water interface was flushed with stream water at peak water velocities. As a result of this advective hyporheic exchange, nighttime oxygen flux increased fourfold with a doubling of water velocity.

The recent discovery that inland waters may store or transform over half of net terrestrial ecosystem production en route to coastal oceans (Cole et al. 2007) has highlighted the contribution of inland waters to global carbon transformation. Low-order streams may be disproportionately important in this regard due to the large surface area that they represent, their high carbon dioxide concentrations, and the high gas transfer velocities that characterize them (Butman and Raymond 2011; Raymond et al. 2013). However, the contribution of in situ organic carbon mineralization to carbon dioxide evasion from streams and rivers is not always well constrained and appears to vary markedly from watershed to watershed. For example, while most of the dissolved organic matter that enters the upper Hudson River is mineralized to CO_2 during transport toward the ocean (Cole and Caraco 2001), in situ mineralization in the Ottawa River may be insignificant (Telmer and Veizer 1999).

Measurements of oxygen flux are integral to our understanding of carbon mineralization in rivers and streams (e.g., Battin et al. 2008) and one of the primary oxygen flux techniques applied to rivers and streams is the open water, or diel change technique (Odum 1956). The technique has been applied to quantify fluvial carbon transformation across biomes and across stream and river orders, where the greatest areal rates of oxygen uptake are observed in small streams (Battin et al. 2008). Because oxygen transformation in the water column of streams is very small relative to benthic rates, benthic flux largely determines stream ecosystem metabolism (Minshall et al. 1983). The vertical flux of oxygen across the sediment–water interface reflects the contributions of oxic metabolic processes and the reaction of oxygen with the reduced products of anoxic metabolic processes. Groundwater inputs, however, can complicate the interpretation of oxygen fluxes. As a result of groundwater inflow, oxygen balances in streams and rivers may reflect not only in situ metabolic processes but also organic carbon mineralization in soils and groundwaters (McCutchan et al. 2002; Hall and Tank 2005).

To improve predictions of organic carbon mineralization in streams and rivers the controls and drivers of aquatic mineralization and primary production need to be better constrained. A proximal driver of metabolism in streams is water velocity (Odum 1956). For cohesive sediments, oxygen consumption is expected to increase linearly with water velocity where the rate of organic matter mineralization is limited by oxygen transport through the diffusive boundary layer (Nakamura and Stefan 1994). For permeable sediments, an

*Correspondence: dirk@email.virginia.edu

increase in overlying water velocity stimulates hyporheic exchange, the advective exchange and mixing of pore water with overlying water. This mechanism is highly efficient in the mineralization of organic carbon (Huettel et al. 2003; Berg et al. 2013) and is one of the primary mechanisms of organic matter mineralization in streams (Grimm and Fisher 1984). Hyporheic exchange scales with sediment permeability and the overlying water velocity squared (Packman and Salehin 2003), and thus varies predictably over stream pools and riffles (Pusch 1996).

The open water technique quantifies oxygen flux under in situ hydrodynamic conditions, but the footprint (the sediment area that contributes to the flux) in streams and rivers is commonly several hundreds to thousands of meters in length (Reichert et al. 2009). The footprint of the open water technique is described according to Reichert et al. (2009) as

$$L_f = \frac{3UH}{k_{O2}} \quad (1)$$

where U is the mean stream velocity (m d^{-1}), H is the mean stream depth (m), and k_{O2} is the gas transfer velocity of oxygen (m d^{-1}). The open water footprint spatially integrates oxygen flux but it may also blur the mechanisms responsible for carbon mineralization at pool, riffle, and run spatial scales. Additionally, the calculation of k_{O2} contributes uncertainty to the overall accuracy of the open water technique (Raymond et al. 2012) even when gas transfer is measured directly by tracer addition (Wanninkhof et al. 1990; McCutchan et al. 1998). Gas tracer addition is also not practical for larger rivers (Marino and Howarth 1993) where alternative techniques for reducing gas transfer uncertainty have been developed (e.g., Holtgrieve et al. 2010).

A recently developed flux technique, aquatic eddy covariance (aka eddy correlation), offers the capability of measuring benthic oxygen fluxes with no gas transfer velocity correction under true in situ hydrodynamic conditions (Berg et al. 2003) and at discrete spatial scales (Berg et al. 2007). Eddy covariance has previously been applied to quantify oxygen flux in rivers (Lorke et al. 2012; Berg et al. 2013; Murniati et al. 2014) and other aquatic environments. In this study we focused on a small coastal stream. The study included two main foci, both of which are novel: the comparison of fluxes and metabolic rates determined with the open water and eddy covariance techniques deployed in parallel, and the effect of stream velocity on benthic oxygen flux determined under true in situ conditions.

Methods

Study site

Rattrap Branch, a second-order stream at the southern end of the Delmarva Peninsula on Virginia's Eastern Shore was selected for this study for its relatively high discharge (commonly 40 L s^{-1}) among seaside streams in the area. The Rattrap Branch watershed is located within the Virginia Coast Reserve—Long Term Ecological Research (VCR-LTER) project area. It is 13 km^2 and is divided between agricultural (38%) and forested lands (41%) with the remainder primarily in low-density residential use (Luckenbach et al. 2008). Rattrap Branch flows through an incomplete forested riparian buffer that exposes most of the stream to direct sunlight for hours at midday. Macrophytes grow densely along the sunlit portions of the reach.

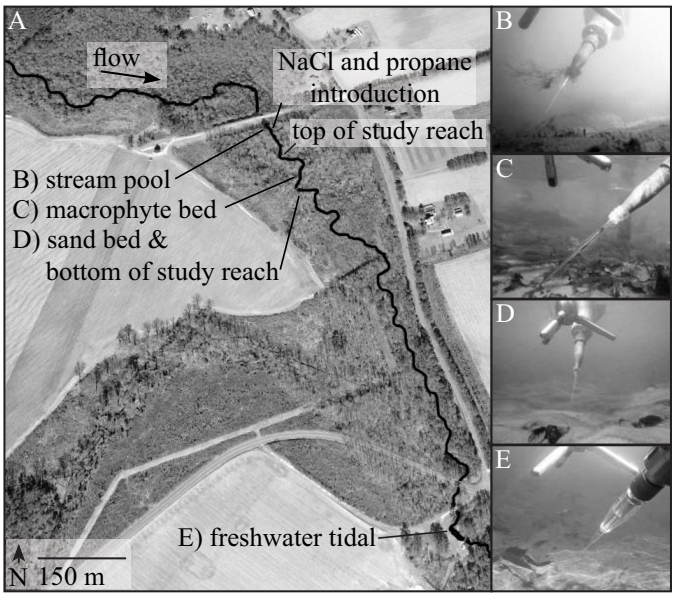

Fig. 1. Map of (A) the Rattrap Branch study site at the southern end of the Delmarva Peninsula, Virginia (37°39′15 N, 75°41′25 W). Aquatic eddy covariance oxygen fluxes were determined at (B) a stream pool, (C) a macrophyte bed, (D) a sand bed, and (E) in a freshwater tidal portion of the stream. Open water fluxes were calculated from water column dissolved oxygen concentrations measured at (D) the bottom of the study reach.

For open water oxygen flux calculations, the gas transfer velocity was determined between the top and bottom of a 100-m study reach (Fig. 1A), while the dissolved oxygen concentration was determined according to the single station technique applied at the bottom of the study reach. Three eddy covariance sites were selected in diverse benthic environments within the open water footprint. According to Eq. 1, we expected the footprint of the open water technique to extend over 100-m upstream of the top of the study reach. The eddy covariance sites included an unvegetated stream pool with cohesive sediments (Fig. 1B), a macrophyte bed (Fig. 1C), and an unvegetated, rippled sand bed (Fig. 1D). Additional eddy covariance measurements were made close to a kilometer downstream of the sand bed site at a freshwater tidal site (Figs. 1A,E). The bed of the tidal site was also permeable, sandy, and unvegetated (Table 1).

Table 1. Overlying water velocities and characteristics of surficial sediments at eddy covariance sites in Rattrap Branch, Virginia. Average current velocities (Velocity) were determined 6 cm above the stream bed ($n = 2$ h). Median particle diameter (D), organic matter content (Organic), permeability (k_s), and chlorophyll *a* content (Chl *a*) were determined in the fall of 2012 (each $n = 3$). Errors refer to standard deviation.

	Velocity (cm s^{-1})	*D* (μm)	Organic (%)	k_s ($\times 10^{-12}$ m^2)	Chl *a* (mg m^{-2})
Stream pool	5.8 ± 2.4	143 ± 105	31.0 ± 4.7	0.5 ± 0.3	29 ± 2
Macrophyte bed	13.4 ± 2.7	375 ± 45	0.3 ± 0.1	12.9 ± 3.9	41 ± 9
Sand bed	16.4 ± 2.6	364 ± 21	0.5 ± 0.1	5.7 ± 1.9	48 ± 10
Tidal site	0.9 − 18.1	351 ± 20	0.8 ± 0.2	5.1 ± 0.4	104 ± 59

Water velocities were greatest at the sand bed and lowest at the pool (Table 1). The median particle size at each of the sites (determined by laser diffraction) was a medium-grained sand (Table 1). The organic matter content was greatest at the pool site (31%, determined by loss on ignition; Table 1). The bulk sediment permeability at the pool site (determined according to Klute and Dirksen 1986) was one-tenth or less that of the other sites (Table 1). Active chlorophyll *a* was present in surficial sediments at all sites (determined according to Pinckney et al. 1994; Table 1).

Aquatic eddy covariance technique

In almost all natural waters, turbulence is the dominant mechanism responsible for the vertical transport of solutes above the sediment–water interface (Boudreau 2001). The eddy covariance technique relies on high frequency (32–64 Hz) measurement of dissolved oxygen and vertical velocity at a point above the sediment–water interface to capture the turbulent fluctuations that facilitate the vertical oxygen flux (Berg et al. 2003). A Nortek Vector acoustic Doppler velocimeter measured the three-dimensional (3D) water velocity in a $\sim 2\,cm^3$ measurement volume and logged the signal output of a custom built submersible amplifier for Clark-type oxygen microsensors (Unisense Ox-eddy sensor; Revsbech 1989). All used oxygen microsensors had a 90% response time of 0.4 s or less. Eddy covariance instruments were mounted on a stainless steel frame, adjustment of which allowed the tip of the microsensor to be aligned a few millimeters downstream of the edge of the Vector's measurement volume. The measurement volume was positioned close to 6-cm above the stream bed.

Eddy covariance flux extraction

Eddy covariance data were collected at 64 Hz and averaged to 16 Hz to reduce noise while keeping the full turbulent signal for data processing. Processing was performed using EddyFlux ver. 2.0 software (Berg, unpubl.). The velocity field was rotated to align its *x*-axis with the mean current to nullify average velocities in both the transverse and vertical axes. The fluctuating components of vertical velocity (u_z') and oxygen (C') were then isolated from their mean values by a Reynolds decomposition. The mean values were determined by least-square linear fitting to the observations in 14.5-min increments (Moncrieff et al. 2004). The benthic oxygen flux was calculated as the mean of the product of the fluctuating components $\overline{u_z'C'}$ (Berg et al. 2003) where the over bar indicates averaging. Uncertainty in eddy covariance oxygen flux was calculated to the first order from the standard deviation of nighttime fluxes, when environmental conditions were relatively stable.

Open water oxygen flux calculation

In parallel, dissolved oxygen flux across the air–water interface was determined with the single station open water technique (Odum 1956; Bott 1996). To quantify the benthic oxygen flux with this technique, a vertical 1D transient mass balance for the water column is applied. The resulting equation, based on Bott (1996), is

$$O_2 \text{ flux} = k_{O2}(O_2 - O_{2\,sat}) + H\frac{dO_2}{dt} \quad (2)$$

where O_2 flux is the vertical flux of oxygen at the sediment–water interface (mmol m^{-2} d^{-1}), O_2 is the observed oxygen concentration in the water column (μmol L^{-1}), and $O_{2\,sat}$ is the oxygen concentration at saturation (μmol L^{-1}; a function of temperature and atmospheric pressure). The dissolved oxygen concentration was determined with optical oxygen sensors (optodes; Hach Environmental) that were calibrated in water saturated air. The optodes also recorded temperature and atmospheric pressure. Additionally, incident photosynthetically active radiation (PAR) at the sediment surface was measured every 0.25 h in the study reach and at eddy covariance sites with submersible PAR sensors (Odyssey). The PAR sensors were calibrated on site, at the sediment surface, to PAR measured with a Li-COR underwater spherical quantum sensor (Long et al. 2012).

Gas transfer velocity

We quantified k_{O2} from the gas transfer velocity of propane (k_{C3H8}; m d^{-1}). Propane (a volatile tracer) and dissolved NaCl (a hydrologic tracer) were introduced continuously, for ~ 1 h, 11 times over the course of this study. The value of k_{C3H8} was quantified from their relative concentration

changes during their transport along the 100-m study reach according to Genereux and Hemond (1992) as

$$k_{C3H8} = \frac{H}{\tau} \ln \frac{G_1 C_2}{G_2 C_1} \quad (3)$$

where τ is the reach travel time (minutes), G is propane concentration (μmol L^{-1}), C is the background-corrected NaCl concentration (μmol L^{-1}) and the subscripts 1 and 2 refer to sample locations at the top and bottom of the study reach. Tracers were introduced 45-m upstream of the top of the study reach (Fig. 1A). The value of τ was determined from the travel time of an introduced NaCl spike. To improve lateral distribution of the tracers upstream of the study reach, NaCl was introduced through a transverse drip line and propane was introduced through a manifold of fine pore ceramic diffusers. Complete lateral mixing of NaCl at the top of the study reach was confirmed and sampling was initiated after the onset of a stable plateau of conductivity readings, typically 20 min after NaCl and propane introduction began. Propane concentrations were quantified on a gas chromatograph equipped with a flame ionization detector. The mean depth in the study reach was calculated from stream discharge (Q_s; m^3 s^{-1}), mean stream velocity (U; m d^{-1}), and mean stream width (W; m), as $H = Q_s\,(UW)^{-1}$. The mean depth was then interpolated over time according to stream stage, determined every 0.25 h using a staff gauge and submerged pressure transducer. Stream discharge was calculated from the plateau concentration of the introduced NaCl tracer at the upstream station according to Roberts et al. (2007) as $Q_s = Q_{inj} C_{inj} (C_1)^{-1}$, where Q_{inj} is the rate of introduction of the NaCl solution and C_{inj} is the NaCl concentration of the solution. The resulting k_{C3H8} included measurements at a stream discharge (Q_s) of 11–63 L s^{-1} and a temperature range of 12–25 °C. We used the 11 calculated values of k_{C3H8} to predict changes in the stream oxygen gas transfer velocity (k_{O2}) across changes in stream discharge and temperature. First, k_{O2} was calculated at a common temperature (17.5 °C; termed k_{600}) from k_{C3H8} according to their Schmidt numbers (Raymond et al., 2012). We used a linear least square regression of k_{600} against stream stage to predict a value of k_{600} for each 0.25-h observation. Based on the stream temperature at each 0.25-h observation, a corresponding k_{O2} was calculated.

We calculated the uncertainty of open water oxygen fluxes with a Monte Carlo simulation (Harmon et al. 2007). Ten thousand independent random samples of each parameter were generated for each reported open water flux from the standard deviations of k_{O2}, H, O_2 and $O_{2\ sat}$. The standard deviation of k_{O2} was determined from confidence intervals on the least square linear regression of k_{O2} against stage ($R^2 = 0.865$, $n = 7$ for 2011 and the spring of 2012; $R^2 = 0.776$, $n = 4$ for the summer and fall of 2012 after a storm-induced stage-discharge shift). The standard deviation of H, 15%, was estimated from the uncertainty of the stream cross-sectional area. The standard deviations of O_2 and $O_{2\ sat}$, each 1%, were determined from the variance of oxygen concentrations recorded by four optodes in the same volume of water. We used the random samples to calculate 10,000 independent oxygen fluxes for each reported value. Their standard deviation was reported as the error estimate for the associated open water flux.

We performed two additional checks to assess the spatial consistency of calculated open water oxygen fluxes in this system. Dual station oxygen fluxes were calculated from the difference in oxygen concentration between the top and bottom of the study reach (Marzolf et al. 1994; Young and Huryn 1998). These were compared with single station calculations made from measurements at the bottom of the study reach. Differences between the dual and single station results were less than 10%. Additionally, for a 2 daytime series, we quantified gas transfer and oxygen flux 100-m and 200-m downstream of the bottom of the study reach. Again, differences between the study reach and the downstream stations were less than 10%.

Ecosystem metabolism

We compared daily gross primary production (GPP), respiration (R), and net ecosystem metabolism (NEM) calculated from eddy covariance oxygen flux at the macrophyte bed and the simultaneous open water oxygen flux. To calculate GPP, R, and NEM, the quarter hourly fluxes were divided into those made in the dark and in light by a threshold of a normalized PAR of 0.01. Respiration (mmol m^{-2} d^{-1}) was calculated according to Hume et al. (2011) as

$$R = \frac{1}{N}\left(\sum \text{flux}_{\text{dark}} + \frac{\sum \text{flux}_{\text{dark}}}{h_{\text{dark}}} h_{\text{light}}\right) \quad (4)$$

where N is the number of 15-min fluxes in 24 h (96), $\text{flux}_{\text{dark}}$ is the flux of oxygen (mmol m^{-2} d^{-1}) recorded in the dark, and h_{dark} and h_{light} are the hours of dark and light, respectively. GPP was calculated as

$$\text{GPP} = \frac{1}{N}\left(\sum \text{flux}_{\text{light}} + \frac{|\sum \text{flux}_{\text{dark}}|}{h_{\text{dark}}} h_{\text{light}}\right) \quad (5)$$

where $\text{flux}_{\text{light}}$ is the flux of oxygen recorded in the light. Similarly, NEM was calculated as

$$\text{NEM} = \frac{1}{N}\left(\sum \text{flux}_{\text{light}} + \sum \text{flux}_{\text{dark}}\right). \quad (6)$$

Groundwater contribution to the open water oxygen flux

Groundwater specific discharge (q_{gw}; m d^{-1}) to the study reach on 11 and 12 May 2011 was calculated from the median dilution of four, hour-long NaCl additions made at similar stream stages. We calculated q_{gw} according to Hall and Tank (2005) as

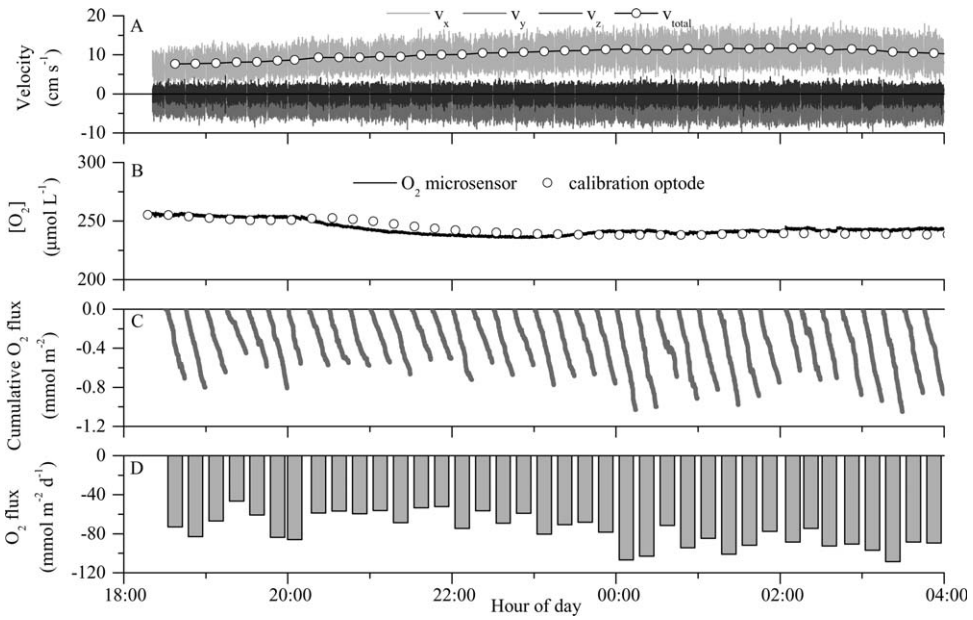

Fig. 2. An example of typical high frequency (16 Hz) eddy covariance data. (A) Three-dimensional water velocities and (B) oxygen concentrations following a storm event on the night of 9 October 2012 at the pool site. (C) The calculated instantaneous oxygen fluxes cumulated over 14.5-min intervals give (D) the reported oxygen fluxes. Note the increase in oxygen flux with the increase in water velocity.

$$q_{gw} = \frac{Q_s}{LW}\left(\frac{C_1 - C_2}{C_2}\right) \quad (7)$$

where L is the length of the study reach (m). The resulting flux of oxygen due to groundwater discharge to the study reach was calculated as

$$O_2 \text{flux}_{gw} = q_{gw}(O_{2\ gw} - O_2) \quad (8)$$

where $O_{2\ gw}$ is the concentration of oxygen in groundwater as it enters the stream. The pore water oxygen concentration was measured at multiple locations at each of the macrophyte bed and sand bed sites. No dissolved oxygen was detected below the sediment surface at a depth of more than 2 cm (Koopmans, unpubl.). Consistent with those observations, groundwater discharge into surface water of Rattrap Branch was assumed to be anoxic.

Velocity-dependent oxygen flux at the tidal site

Additional eddy covariance measurements were made in October of 2012 in the freshwater tidal portion of Rattrap Branch. To simplify interpretation of the relationship between water velocity and oxygen flux only nighttime fluxes at this site are presented. Supplementary observations of the velocity-dependent flushing of surficial pore waters were made by burying an optode (Precision Measurement Engineering) in the stream bed so that the optode membrane was perpendicular to the flow direction and the sensing surface was ~ 1.5-cm below the sand–water interface.

Results

Comparison of eddy covariance and open water oxygen fluxes

The footprint of the eddy covariance technique was an ellipse about 1-m wide and 10-m long according to first-order estimates from Berg et al. (2007) and was aligned with the predominant flow direction along the center of the channel. The footprint of the open water technique, in contrast, averaged 500 m in the spring of 2011 and 2012 (Eq. 1). An example of eddy covariance data, and the oxygen fluxes derived from them, are given in Fig. 2.

Nighttime oxygen uptake determined with the eddy covariance technique was always smaller than open water oxygen uptake. For example, at the pool site between 3 and 4 May 2012, the eddy covariance oxygen flux overnight (-27 ± 7 mmol m^{-2} d^{-1}, $n = 27$) was 23-fold smaller than open water oxygen flux (-631 ± 105 mmol m^{-2} d^{-1}, $n = 27$; Figs. 3A,B). Daytime eddy covariance oxygen flux at the pool peaked in direct sunlight at 62 mmol m^{-2} d^{-1} (Fig. 3A), decreased sharply in the afternoon shade of the forest canopy to -66 mmol m^{-2} d^{-1}, then diminished to a similar rate (-26 ± 8 mmol m^{-2} d^{-1}, $n = 13$) to that of the prior night. Daytime open water oxygen flux peaked at 430 mmol m^{-2} d^{-1} but remained positive throughout the afternoon (Fig. 3B). Storage of oxygen in the water column was small compared to the benthic flux (Fig. 3B); as a result, according to Eq. 2, uncertainty in open water oxygen flux is limited primarily to uncertainty in k_{O2}.

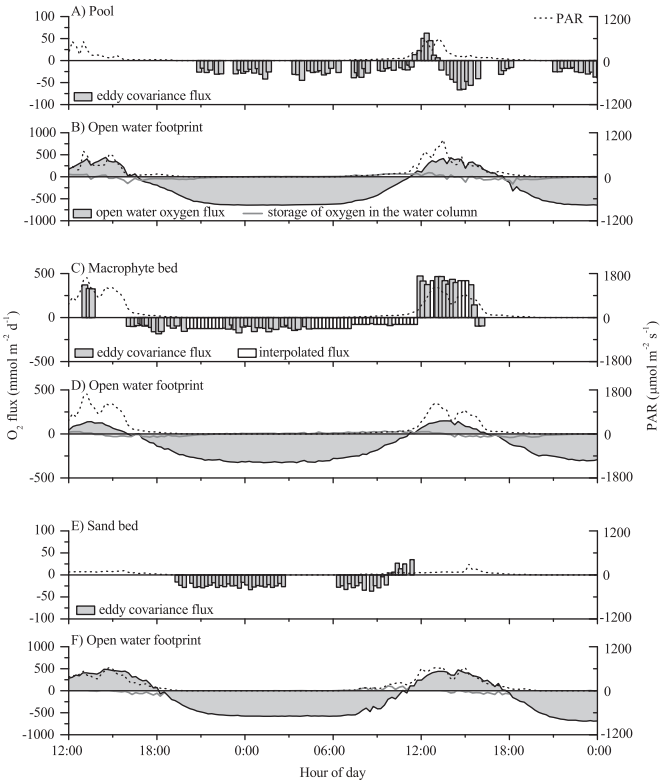

Fig. 3. Time series of eddy covariance and open water oxygen fluxes with PAR on 3 and 4 May 2012 at (A) the pool and (B) in the open water footprint; on 11 and 12 May 2011 at (C) the macrophyte bed and (D) in the open water footprint; and on 30 April and 1 May 2012 at (E) the sand bed and (F) in the open water footprint. A positive flux represents benthic oxygen production. Note the order of magnitude differences in oxygen flux between (A) and (B), also (E) and (F). Eddy covariance oxygen fluxes at (C) include data gaps caused by debris at the microsensor tip. These gaps were filled by interpolation between known fluxes to calculate the daily metabolic rate.

At the macrophyte bed site, in contrast, eddy covariance oxygen fluxes were similar in magnitude to open water oxygen fluxes. For example, between 11 and 12 May 2012, the eddy covariance oxygen flux overnight (-125 ± 27 mmol m^{-2} d^{-1} $n = 23$; Fig. 3C) was 2.5-fold smaller than open water oxygen flux measured at the same time (-315 ± 55 mmol m^{-2} d^{-1} $n = 23$, Fig. 3D). In direct sunlight, however, the pattern was reversed with eddy covariance oxygen flux at the macrophyte bed (425 ± 38 mmol m^{-2} d^{-1}, $n = 9$) threefold greater than open water oxygen flux (136 ± 34 mmol m^{-2} d^{-1}, $n = 9$). The sand bed site was similar to the pool site, where eddy covariance oxygen fluxes were small relative to open water oxygen fluxes. For example, between 30 April and 1 May 2012, the nighttime eddy covariance oxygen flux (-25 ± 4 mmol m^{-2} d^{-1}, $n = 29$; Fig. 3E) was 20-fold smaller than open water oxygen flux (-536 ± 96 mmol m^{-2} d^{-1}, $n = 29$; Fig. 3F). No midday eddy covariance oxygen fluxes were determined at this site; the higher water velocities there caused extensive accumulation of debris on the microsensors and made eddy covariance measurements difficult. All eddy covariance fluxes from each of the three sites were paired with simultaneous open water fluxes for comparison across days and seasons (Fig. 4). The results were generally similar to those found at finer temporal scales (Fig. 3). These patterns also generally persisted within 24 h after rain events when open water oxygen uptake exceeded eddy covariance oxygen uptake by 16- and 6-fold at the pool and sand bed (Figs. 4A,C) but by twofold at the macrophyte bed (Fig. 4B).

Ecosystem metabolism

At the macrophyte bed on 11 and 12 May 2011, NEM calculated with the eddy covariance technique was close to a metabolic balance while open water NEM was highly heterotrophic (Fig. 5). Eddy covariance R (-125 ± 24 mmol O_2 m^{-2} d^{-1}) was 2.5-fold smaller than open water R (-306 ± 54 mmol O_2 m^{-2} d^{-1}) but eddy covariance GPP (92 ± 26 mmol O_2 m^{-2} d^{-1}) was 1.5-fold smaller than open water GPP (136 ± 54 mmol O_2 m^{-2} d^{-1}). The resulting eddy covariance NEM (-32 ± 26 mmol O_2 m^{-2} d^{-1}) was fivefold smaller than the open water NEM (-170 ± 54 mmol O_2 m^{-2} d^{-1}). The large uncertainty in open water measurements was due primarily to k_{O2} and H.

The estimated oxygen flux due to anoxic groundwater discharge accounted for 40% of the nighttime open water oxygen uptake (Fig. 5). If groundwater entered the stream in lateral flow through the banks of the stream, the effect of groundwater discharge may not be included in eddy covariance oxygen flux. To examine this hypothesis, the groundwater correction (Eq. 8) was applied to the open water oxygen flux. According to Eq. 7, groundwater discharge to the study reach was 4.3% of Q_s, or 0.47 m d^{-1}. The oxygen flux generated by anoxic groundwater discharge at night (-126 mmol O_2 m^{-2} d^{-1}) was smaller than during the day (-144 mmol O_2 m^{-2} d^{-1}) because of the diurnal variation in dissolved oxygen concentration in the stream. After subtracting the groundwater contribution, open water R decreased by 40% and GPP increased by 6% to rates 1.4- and 1.6-fold greater than eddy covariance R and GPP. Open water NEM calculated without the estimated contribution of anoxic groundwater (-33 ± 74 mmol O_2 m^{-2} d^{-1}) was close to NEM calculated with the eddy covariance technique at the macrophyte bed (-32 ± 26 mmol O_2 m^{-2} d^{-1}) but included substantial uncertainty (Fig. 5).

Velocity effect on oxygen flux

On the night of 9 October 2012, following a storm event, water velocities at the pool site increased from 7.7 cm s^{-1} to a maximum of 11.7 cm s^{-1} (Fig. 2A). Oxygen uptake increased from approximately -70 mmol O_2 m^{-2} d^{-1} to -90 mmol O_2 m^{-2} d^{-1} with the increase in water velocity (Fig. 2D; $R^2 = 0.60$, $p < 0.05$, $n = 38$). The effect of changes in water velocity on oxygen flux was examined further at the

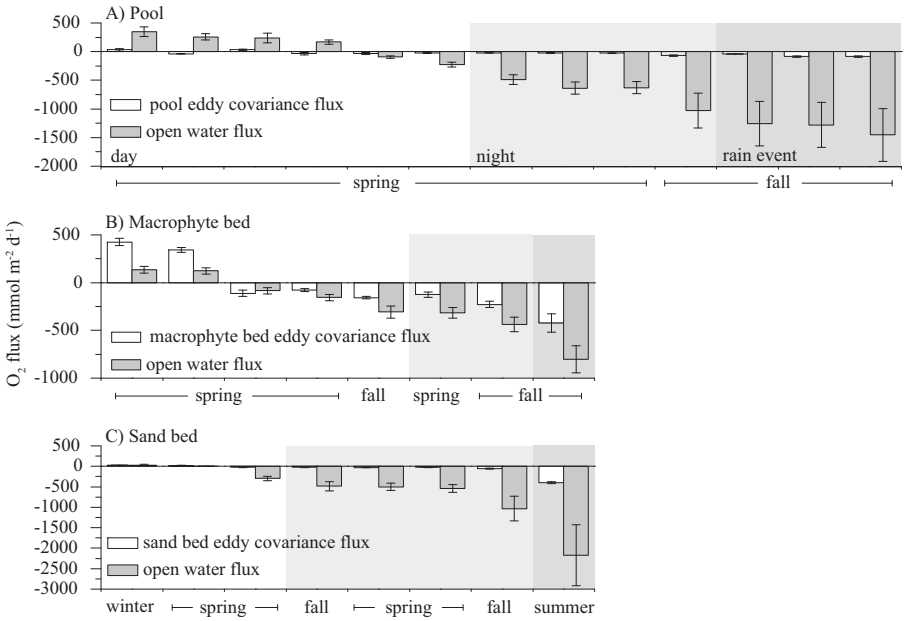

Fig. 4. All eddy covariance fluxes at (A) the pool, (B) the macrophyte bed, and (C) the sand bed paired with simultaneous open water oxygen fluxes and ranked by their magnitude (mean of 136 ± 20 min, $n = 29$). Measurement during the day, at night, within 24 h of rain events, and by season are indicated. Eddy covariance oxygen fluxes only exceeded open water fluxes during the day at the macrophyte bed.

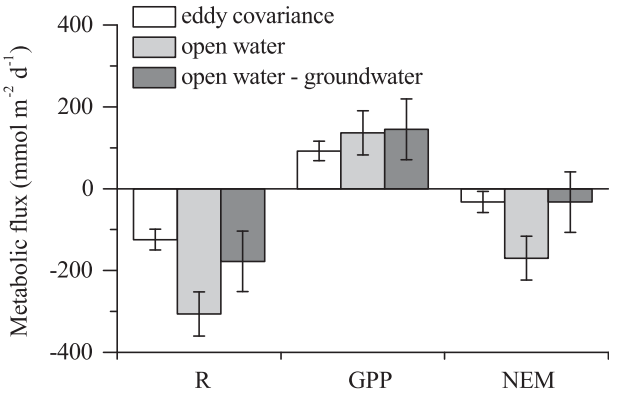

Fig. 5. Metabolic respiration (R), gross primary production (GPP), and net ecosystem metabolism (NEM) on 11 and 12 May 2011 calculated from the eddy covariance oxygen flux at the macrophyte bed and from the simultaneous open water oxygen flux. The oxygen flux due to anoxic groundwater discharge to the study reach was also calculated and subtracted from the open water oxygen flux (open water—groundwater).

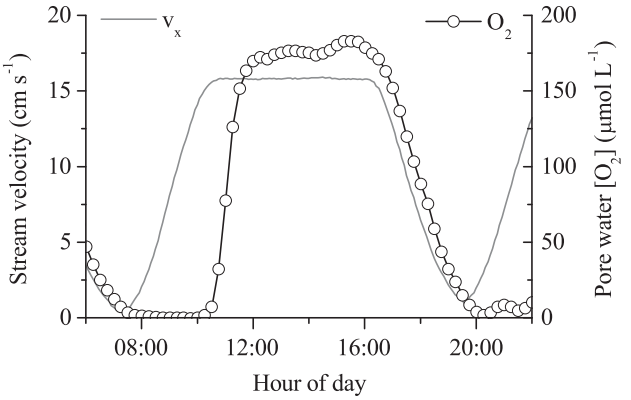

Fig. 6. Tidal current-induced flushing of surficial sands in the freshwater tidal portion of Rattrap Branch on 22 October 2012. A linear decrease in dissolved oxygen in pore water was observed between 17:00 and 19:00. This decrease was used to produce a first order volumetric oxygen consumption rate.

tidal site, where an increase in water velocity caused the flushing of surficial pore waters (Fig. 6). As tidal water velocities approached a sustained peak of 16 cm s^{-1}, pore water at the site was mixed with overlying water and the oxygen concentration in surficial pore water increased from 0 to 165 μmol L^{-1}. Hours later water velocities slowed and the dissolved oxygen concentration in pore water decreased again. Assuming that pore water mixing ceased, this decrease in dissolved oxygen can be translated to a volumetric rate of oxygen consumption. Assuming further that the rate of change in oxygen concentration occurred to a depth of 1.5 cm it would, to the first order, correspond to an oxygen uptake of −20 mmol m^{-2} d^{-1}.

The small rate of oxygen uptake determined from changes in dissolved oxygen in pore water at the tidal site agreed with nighttime oxygen uptake measured with eddy covariance at

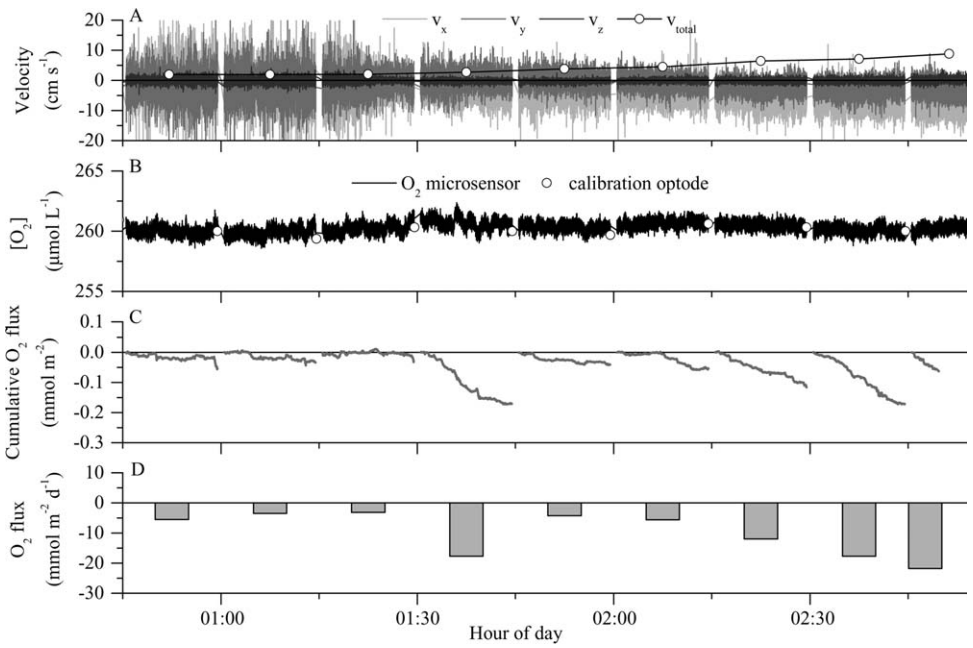

Fig. 7. Eddy covariance oxygen flux at the tidal site on 21 October 2012. (A–D) Same as Fig. 2. Oxygen uptake increased with increasing water velocity. A lack of particles in suspension at low flow caused elevated noise in the velocity observations prior to 01:30.

the site. During eddy covariance measurements, water velocities ranged from less than 2 cm s^{-1} to 9 cm s^{-1} (Fig. 7A). Oxygen concentrations in the water column were unchanged (Fig. 7B) but oxygen uptake increased with water velocity (Figs. 7C,D). While the water velocity was less than 2 cm s^{-1}, oxygen flux was a small but identifiable −4 mmol m^{-2} d^{-1} (Fig. 7D). As water velocity increased to 3 cm s^{-1}, a transient peak in oxygen uptake occurred (Figs. 7C,D, between 01:30 h and 01:45 h). As the water velocity increased further, oxygen uptake increased steadily from −4 mmol m^{-2} d^{-1} to a maximum of −22 mmol m^{-2} d^{-1} (Fig. 7D). This same pattern, including the transient peak in oxygen uptake at a water velocity close to 3 cm s^{-1}, occurred again on a subsequent night (Fig. 8). The transient peak was consistent with the mixing of a hypoxic portion of the diffusive boundary layer into the overlying water column. A flux of this magnitude (−18 mmol m^{-2} d^{-1} for 0.25 h) would require the mixing of an anoxic layer ~ 0.5-mm thick. At water velocities between 4 cm s^{-1} and 9 cm s^{-1}, oxygen fluxes were correlated with velocity ($R^2 = 0.83$, $p < 0.001$) and increased fourfold with the doubling of velocity (Fig. 8).

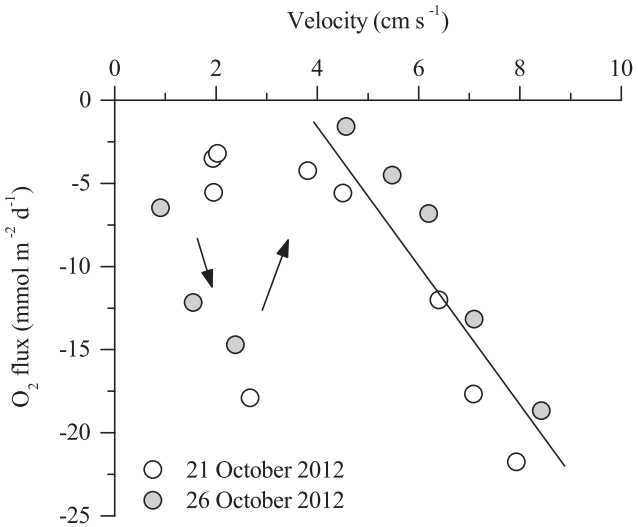

Fig. 8. Eddy covariance oxygen fluxes at the tidal site on 21 and 26 October 2012. Arrows indicate the flux sequences in time.

Discussion

Attributes of eddy covariance oxygen fluxes

The open water technique (Odum 1956) offers the advantage of a "whole ecosystem" measure of benthic oxygen flux from which whole system daily values of stream and river metabolism (R, GPP, and NEM) can be derived. Because drift in dissolved oxygen measured by modern commercial optodes is small, open water fluxes can be quantified in a river or stream continually for years (Roberts et al. 2007). The measured fluxes, however, may incorporate significant uncertainties (Wanninkhof et al. 1990; McCutchan et al. 1998). The gas transfer velocity and mean stream depth must be determined. Errors in each, including their changes with stream stage, transfer proportionally to errors in flux (Raymond et al. 2012). With eddy covariance, in contrast, oxygen flux is determined with high temporal resolution over a well-defined footprint without knowledge of the gas transfer velocity (Berg et al. 2003, 2007). However,

limitations to fast-responding oxygen sensors may limit continuous benthic flux measurements to a maximum of about 1 d. As a result, the eddy covariance and open water techniques should be viewed as highly complementary for studies of fluvial benthic fluxes and metabolism.

An example of the advantages of the discrete footprint and the high temporal resolution of eddy covariance can be seen in the effects of velocity on oxygen flux. At the pool site, an increase in oxygen uptake was observed with an increase in water velocity (Fig. 2). The mechanisms responsible may include velocity driven hyporheic exchange (Huettel et al. 2003), increased supply of particulate and dissolved organic carbon (Buffam et al. 2001), as well as increased hypoxic groundwater inflow. At the tidal site, the eddy covariance technique could be used to quantify the effect of an increase in velocity with minimal contribution of other factors, measurements that would not be possible with the open water technique. The increase in oxygen consumption as water velocities increased from 4 cm s^{-1} to 9 cm s^{-1} (Fig. 8) was consistent with a limitation of carbon mineralization by the rate of pore water exchange. This effect has been observed in manipulated flux chambers deployed in streams (Hickey 1988) but this is the first time, to the best of our knowledge, the effect has been quantified in a stream using in situ data. Recently, similar responses have been measured with eddy covariance in coastal permeable sediments (Hume et al. 2011; Berg et al. 2013) and in an impounded river (Lorke et al. 2012).

The eddy covariance technique also resolved abrupt, light dependent changes in oxygen flux at each of the pool, macrophyte bed, and sand bed (Figs. 3A,C,E) but similar changes in oxygen flux were not resolved with the open water technique. At the pool site, the peak eddy covariance oxygen uptake in the early afternoon shade (-66 mmol m^{-2} d^{-1}) was more than double the nighttime average (-27 mmol m^{-2} d^{-1}; Fig. 3A). This pattern is consistent with limited observations that during day, benthic oxygen uptake may be enhanced due to the additional mineralization of recently produced, highly labile photosynthates in streams and rivers (Kaplan and Bott 1983). The availability of photosynthates may be important in fueling rates of aquatic ecosystem respiration (Baines and Pace 1991).

Comparison between eddy covariance sites

Spring nighttime oxygen uptake at the macrophyte bed was fivefold greater than at the pool or sand bed. Most of that difference can likely be attributed to vegetation and associated epiphytes. Eddy covariance oxygen production reached 400 mmol m^{-2} d^{-1} during the day and averaged -125 mmol m^{-2} d^{-1} at night (Fig. 3C). This contrasted with the unvegetated pool where daytime oxygen production briefly peaked at 62 mmol m^{-2} d^{-1} and at night averaged -27 mmol m^{-2} d^{-1} (Fig. 3A). At the unvegetated sand bed nighttime oxygen flux averaged -25 mmol m^{-2} d^{-1} (Fig. 3E). The high rates of nighttime oxygen consumption and production at the macrophyte bed and comparative low rates at the other sites suggest that both production and consumption of oxygen in the stream were associated with vegetation. These results support evidence that respiration is tightly coupled to primary production in streams and rivers (Townsend et al. 2011; Dodds et al. 2013). Similarly, R and GPP were also coupled in eddy covariance measurements over vegetated sites in marine systems (Hume et al. 2011; Rheuban et al. 2014). These observations contrast with the decoupling of R from GPP observed with open water oxygen flux measurement in lowland New Zealand streams (O'Brien et al. 2013) and in a survey of 26 streams in North America (Sinsabaugh 1997). The discrepancy may be explained by the observation that much of the carbon mineralized in streams is allochthonous in origin (Battin et al., 2008), however, a contributing explanation may also be that open water oxygen fluxes in streams are more commonly biased by proportionally high rates of groundwater inflow (McCutchan et al. 2002; Hall and Tank 2005).

The sand bed and pool sites exhibited similar oxygen fluxes diurnally and across seasons (Figs. 3 and 4) despite their contrasting organic matter contents (0.5% and 31%, Table 1) and contrasting sediment permeabilities (5.7×10^{-12} m^2 and 0.5×10^{-12} m^2, Table 1). These results suggest that in this stream advection-driven organic carbon mineralization in permeable sediments can be of the same order as diffusion-facilitated carbon mineralization in cohesive sediments (i.e., permeability $< 10^{-12}$ m^2; Huettel et al. 2003). In explanation, while stream flow in the short term can modulate oxygen uptake, labile organic matter supply ultimately limits rates of respiration (Baines and Pace 1991; Gudasz et al. 2012). It is possible that the supply of labile organic matter to the sand bed and pool sites is similar. This point is valid over longer time scales but over shorter time scales benthic oxygen flux clearly responds to changes in flow. Oxygen flux at the tidal site demonstrates this with an uptake of -3 mmol m^{-2} d^{-1} at 2 cm s^{-1}, but -22 mmol m^{-2} d^{-1} at 8 cm s^{-1} (Fig. 8).

Comparison between the eddy covariance and open water techniques

The footprint of the eddy covariance technique was much shorter and narrower (about 10-m long and 1-m wide) than the open water footprint (about 500-m long and bank-to-bank). Substantial differences between eddy covariance and open water oxygen fluxes were observed. Nighttime eddy covariance uptake at the pool and sand bed were 23-fold and 20-fold smaller than the concurrent open water oxygen uptake. Daytime oxygen production at the pool site was also insignificant relative to open water oxygen production (Fig. 4A). Assuming that the open water flux was composed of highly variable fluxes from different substrates, the benthic oxygen fluxes at the pool and sand bed did not contribute substantially to it. The site that agreed most closely with open water fluxes was the macrophyte bed. At that site, eddy

covariance GPP (92 ± 26 mmol m^{-2} d^{-1}) was relatively similar in magnitude to open water GPP (136 ± 54 mmol m^{-2} d^{-1}), but eddy covariance *R* (125 ± 24 mmol m^{-2} d^{-1}) was less than half of open water *R* (306 ± 54 mmol m^{-2} d^{-1}; Fig. 5). We suggest that uncertainty in the measurement of the gas transfer velocity and its variation over time does not explain this difference; for open water *R* to agree with eddy covariance *R*, both sample means would have to be in error by more than two sample standard deviations. Instead, it is likely that the open water footprint incorporated metabolic processes that consumed substantially more oxygen than occurred in the eddy covariance footprint at the macrophyte bed. However, during this study, we quantified oxygen uptake at diverse benthic sites with organic-rich sediments (pool), rippled sand beds with fast overlying flow (sand bed; Table 1), and at a sand bed with hyporheic exchange (tidal site; Figs. 6 and 8). The rate of oxygen uptake at these unvegetated sites was fivefold smaller than oxygen uptake at the macrophyte bed, suggesting that benthic organic matter mineralization at alternate sites within the open water footprint may not explain the difference.

Groundwater discharge, however, can account for the difference between eddy covariance at the macrophyte bed and open water oxygen flux. Groundwater discharge through submerged stream banks and at the stream margins was identified as the primary flow path to Cobb Mill Creek (Gu et al. 2008), a similar sand bed stream in the VCR-LTER project area. This explanation is supported by observation of greater horizontal than vertical hydraulic conductivities in river alluvia (Chen 2000), and by substantial lateral exchange between streams and alluvial aquifers (Gunduz and Aral 2005). After subtracting the estimated oxygen flux due to groundwater inflow, the open water and eddy covariance values of NEM agreed (Fig. 5). The calculated groundwater discharge to the study reach (0.47 m d^{-1}) matched roughly the rate determined by Hall and Tank (2005) in 11 streams (0.45 m d^{-1}). Furthermore, the assumption of anoxic groundwater discharge based on point measurements (e.g., Fig. 6, and Koopmans, unpubl.) is supported by efficient denitrification in lateral groundwater flow paths in Cobb Mill Creek (Gu et al., 2008). Given this explanation, the location of dissolved oxygen removal from groundwater is important. If it occurs in the final meter of flow through streambed sediments (Gu et al. 2007), then this effect may be correctly attributed to stream ecosystem metabolism. Farther from the stream in alluvial aquifers, however, it may be appropriate to classify it as terrestrial ecosystem metabolism. Adding to this substantial effect (Fig. 5), anoxic groundwater may also deliver reduced groundwater-born constituencies such as Fe^{2+}, Mn^{2+}, and the organic products of fermentative reactions. The oxidation of these constituencies in surface waters would further contribute to open water oxygen uptake. To our knowledge, these processes have not been fully recognized as a contributor to open water oxygen flux.

References

Baines, S. B., and M. L. Pace. 1991. The production of dissolved organic matter by phytoplankton and its importance to bacteria: patterns across marine and freshwater systems. Limnol. Oceanogr. **36**: 1078–1090. doi:10.4319/lo.1991.36.6.1078

Battin, T. J., and others. 2008. Biophysical controls on organic carbon fluxes in fluvial networks. Nat. Geosci. **1**: 95–100. doi:10.1038/ngeo101

Berg, P., H. Røy, F. Janssen, V. Meyer, B. B. Jørgensen, M. Huettel, and D. De Beer. 2003. Oxygen uptake by aquatic sediments measured with a novel non-invasive eddy-correlation technique. Mar. Ecol. Prog. Ser. **261**: 75–83. doi:10.3354/meps261075

Berg, P., H. Røy, and P. L. Wiberg. 2007. Eddy correlation flux measurements: The sediment surface area that contributes to the flux. Limnol. Oceanogr. **52**: 1672–1684. doi:10.4319/lo.2007.52.4.1672

Berg, P., and others. 2013. Eddy covariance measurements of oxygen fluxes in permeable sediments exposed to varying current flow and light. Limnol. Oceanogr. **58**: 1329–1343. doi:10.4319/lo.2013.58.4.1329

Boudreau, B. P. 2001. Solute transport above the sediment-water interface, p. 104–123. *In* B. P. Boudreau and B. B. Jørgensen [eds.], The benthic boundary layer. Oxford Univ. Press.

Bott, T. L. 1996. Primary productivity and community respiration, p. 533-556. *In* F. R. Hauer and G. A. Lamberti [eds.], Methods in stream ecology. Academic Press.

Buffam, I., J. N. Galloway, L. K. Blum, and K. J. McGlathery. 2001. A stormflow/baseflow comparison of dissolved organic matter concentrations and bioavailability in an Appalachian stream. Biogeochemistry **53**: 269–306. doi:10.1023/A:1010643432253

Butman, D., and P. A. Raymond. 2011. Significant efflux of carbon dioxide from streams and rivers in the United States. Nat. Geosci. **4**: 839–842. doi:10.1038/ngeo1294

Chen, X. 2000. Measurement of streambed hydraulic conductivity and its anisotropy. Environ. Geol. **39**: 1317–1324. doi:10.1007/s002540000172

Cole, J. J., and N. F. Caraco. 2001. Carbon in catchments: connecting terrestrial carbon losses with aquatic metabolism. Mar. Freshw. Res. **52**: 101–110. doi:10.1071/MF00084

Cole, J. J., and others. 2007. Plumbing the global carbon cycle: integrating inland waters into the terrestrial carbon budget. Ecosystems **10**: 172–184. doi:10.1007/s10021-006-9013-8

Dodds, W. K., A. M. Veach, C. M. Ruffing, D. M. Larson, J. L. Fischer, and K. H. Costigan. 2013. Abiotic controls and temporal variability of river metabolism: multiyear analyses of Mississippi and Chattahoochee River data. Freshw. Sci. **32**: 1073–1087. doi:10.1899/13-018.1

Genereux, D. P., and H. F. Hemond. 1992. Determination of gas exchange rate constants for a small stream on Walker Branch

watershed, Tennessee. Wat. Resour. Res. **28**: 2365-2374. doi:10.1029/92WR01083

Grimm, N. B., and S. G. Fisher. 1984. Exchange between interstitial and surface water: implications for stream metabolism and nutrient cycling. Hydrobiologia **111**: 219–228. doi:10.1007/BF00007202

Gu, C., G. M. Hornberger, J. S. Herman, and A. L. Mills. 2008. Influence of stream-groundwater interactions in the streambed sediments on NO_3^- flux to a low-relief coastal stream. Wat. Resour. Res. **44**: W11432. doi:10.1029/2007WR006739

Gu, C., G. M. Hornberger, A. L. Mills, J. S. Herman, and S. A. Flewelling. 2007. Nitrate reduction in streambed sediments: Effects of flow and biogeochemical kinetics. Wat. Resour. Res. **43**: W12413. doi:10.1029/2007WR006027

Gudasz, C., D. Bastviken, K. Premke, K. Steger, and L. J. Tranvik. 2012. Constrained microbial processing of allochthonous organic carbon in boreal lake sediments. Limnol. Oceanogr. **57**: 163-175. doi:10.4319/lo.2012.57.1.0163

Gunduz, O., and M. M. Aral. 2005. River networks and groundwater flow: a simultaneous solution of a coupled system. J. Hydrol. **301**: 216–234. doi:10.1016/j.jhydrol.2004.06.034

Hall, R. O., and J. L. Tank. 2005. Correcting whole-stream estimates of metabolism for groundwater input. Limnol. Oceanogr.: Methods **3**: 222–229. doi:10.4319/lom.2005.3.222

Harmon, M. E., D. L. Phillips, J. J. Battles, A. Rassweiler, R. O. Hall, and W. K. Lauenroth. 2007. Quantifying uncertainty in net primary production measurements, p. 238–260. *In* T. J. Fahey and A. K. Knapp [eds.], Principles and standards for measuring net primary production in long-term ecological studies. Oxford Univ. Press.

Hickey, C. W. 1988. Benthic chamber for use in rivers: testing against oxygen mass balances. J. Environ. Eng. **114**: 828–845. doi:10.1061/(ASCE)0733-9372(1988)114:4(828)

Holtgrieve, G. W., D. E. Schindler, T. A. Branch, and Z. Teresa A'mar. 2010. Simultaneous quantification of aquatic ecosystem metabolism and reaeration using a Bayesian statistical model of oxygen dynamics. Limnol. Oceanogr. **55**: 1047-1063. doi:10.4319/lo.2010.55.3.1047

Huettel, M., H. Røy, E. Precht, and S. Ehrenhauss. 2003. Hydrodynamical impact on biogeochemical processes in aquatic sediments. Hydrobiologia **494**:231-236. doi:10.1007/978-94-017-3366-3_31

Hume, A. C., P. Berg, and K. J. McGlathery. 2011. Dissolved oxygen fluxes and ecosystem metabolism in an eelgrass (*Zostera marina*) meadow measured with the eddy correlation technique. Limnol. Oceanogr. **56**: 86-96. doi:10.4319/lo.2011.56.1.0086

Kaplan, L., and T. L. Bott. 1983. Microbial heterotrophic utilization of dissolved organic matter in a piedmont stream. Freshw. Biol. **13**: 363–377. doi:10.1111/j.1365-2427.1983.tb00686.x

Klute, E. A., and C. Dirksen. 1986. Hydraulic conductivity and diffusivity: Laboratory methods, p. 687–734. *In* E. A. Klute [ed.], Methods of soil analysis: part 1—physical and mineralogical methods. American Society of Agronomy-Soil Science Society of America.

Long, M. H., J. E. Rheuban, P. Berg, and J. C. Zieman. 2012. A comparison and correction of light intensity loggers to photosynthetically active radiation sensors. Limnol. Oceanogr.: Methods **10**: 416–424. doi:10.4319/lom.2012.10.416

Lorke, A., D. F. McGinnis, A. Maeck, and H. Fischer. 2012. Effect of ship locking on sediment oxygen uptake in impounded rivers. Wat. Resour. Res. **48**:W12514. doi:10.1029/2012WR012483

Luckenbach, M., P. Ross, and A. Curry. 2008. Evaluating the relationship between impervious surfaces within watersheds and coastal water quality on Virginia's Eastern Shore. Report to the Virginia Coastal Zone Management Program, Virginia Department of Environmental Quality, Richmond, VA.

Marino, R., and R. W. Howarth. 1993. Atmospheric oxygen exchange in the Hudson River: dome measurements and comparison with other natural waters. Estuaries **16**: 433–445. doi:10.2307/1352591

Marzolf, E. R., P. J. Mulholland, and A. D. Steinman. 1994. Improvements to the diurnal upstream-downstream dissolved oxygen change technique for determining whole-stream metabolism in small streams. Can. J. Fish. Aquat. Sci. **51**: 1591–1599. doi:10.1139/f94-158

McCutchan, J. H., W. M. Lewis, and J. F. Saunders. 1998. Uncertainty in the estimation of stream metabolism from open-channel oxygen concentrations. J. North Am. Benthol. Soc. **17**:155-164. doi:10.2307/1467959

McCutchan, J. H., J. F. Saunders, W. M. Lewis, and M. G. Hayden. 2002. Effects of groundwater flux on open-channel estimates of stream metabolism. Limnol. Oceanogr. **47**: 321–324. doi:10.4319/lo.2002.47.1.0321

Minshall, G. W., R. C. Petersen, K. W. Cummins, T. L. Bott, J. R. Sedell, C. E. Cushing, and R. L. Vannote. 1983. Interbiome comparison of stream ecosystem dynamics. Ecol. Monogr. **53**: 1–25. doi:10.2307/1942585

Moncrieff, J., R. Clement, J. Finnigan, and T. Meyers. 2004. Averaging, detrending, and filtering of eddy covariance time series, p. 7-31. *In* X. Lee, W. Massman and B. Law [eds.], Handbook of micrometeorology—a guide for surface flux measurement and analysis. Atmospheric and Oceanographic Sciences Library. Kluwer.

Murniati, E., S. Geissler, and A. Lorke. 2014. Short-term and seasonal variability of oxygen fluxes at the sediment-water interface in a riverine lake. Aquat. Sci. doi:10.1007/s00027-014-0362-7

Nakamura, Y., and H. G. Stefan. 1994. Effect of flow velocity on sediment oxygen demand: Theory. J. Environ. Eng. ASCE **120**: 996–1016. doi:10.1061/(ASCE)0733-9372(1994)120:5(996)

O'Brien, J. M., J. L. Lessard, D. Plew, S. E. Graham, and A. R. McIntosh. 2013. Aquatic macrophytes alter metabolism and nutrient cycling in lowland streams. Ecosystems **17**: 405–417. doi:10.1007/s10021-013-9730-8

Odum, H. T. 1956. Primary production in flowing waters. Limnol. Oceanogr. **1**: 102–117. doi:10.4319/lo.1956.1.2.0102

Packman, A. I., and M. Salehin. 2003. Relative roles of stream flow and sedimentary conditions in controlling hyporheic exchange. Hydrobiologia. **494**: 291–297. doi:10.1007/978-94-017-3366-3_40

Pinckney, J., R. Papa, and R. Zingmark. 1994. Comparison of high-performance liquid chromatographic, spectrophotometric, and fluorometric methods for determining chlorophyll *a* concentrations in estuarine sediments. J. Microbiol. Meth. **19**: 59–66. doi:10.1016/0167-7012(94)90026-4

Pusch, M. 1996. The metabolism of organic matter in the hyporheic zone of a mountain stream, and its spatial distribution. Hydrobiologia **323**: 107–118. doi:10.1007/BF00017588

Raymond, P. A., and others. 2012. Scaling the gas transfer velocity and hydraulic geometry in streams and small rivers. Limnol. Oceanogr.: Fluids Environ. **2**: 41–53. doi:10.1215/21573689-1597669

Raymond, P. A., and others. 2013. Global carbon dioxide emissions from inland waters. Nature **503**: 355–359. doi:10.1038/nature12760

Reichert, P., U. Uehlinger, and V. Acuña. 2009. Estimating stream metabolism from oxygen concentrations: effect of spatial heterogeneity. J. Geophys. Res. Biogeo. **114**: G03016. doi:10.1029/2008JG000917

Revsbech, N. P. 1989. An oxygen microsensor with a guard cathode. Limnol. Oceanogr. **34**: 474–478. doi:10.4319/lo.1989.34.2.0474

Rheuban, J. E., P. Berg, and K. J. McGlathery. 2014. Multiple timescale processes drive ecosystem metabolism in eelgrass (*Zostera marina*) meadows. Mar. Ecol. Prog. Ser. **507**:1-13. doi:10.3354/meps10843

Roberts, B. J., P. J. Mulholland, and W. R. Hill. 2007. Multiple scales of temporal variability in ecosystem metabolism rates: results from 2 years of continuous monitoring in a forested headwater stream. Ecosystems **10**: 588–606. doi:10.1007/s10021-007-9059-2

Sinsabaugh, R. L. 1997. Large-scale trends for stream benthic respiration. J. North Am. Benthol. Soc. **16**: 119–122. doi:10.2307/1468244

Telmer, K., and J. Veizer. 1999. Carbon fluxes, pCO_2 and substrate weathering in a large northern river basin, Canada: carbon isotope perspectives. Chem. Geol. **159**: 61–86. doi:10.1016/S0009-2541(99)00034-0

Townsend, S. A., I. T. Webster, and J. H. Schult. 2011. Metabolism in a groundwater-fed river system in the Australian wet/dry tropics: tight coupling of photosynthesis and respiration. J. North Am. Benthol. Soc. **30**: 603–620. doi:10.1899/10-066.1

Wanninkhof, R., P. J. Mulholland, and J. W. Elwood. 1990. Gas exchange rates for a first-order stream determined with deliberate and natural tracers. Wat. Resour. Res. **26**: 1621–1630. doi:10.1029/WR026i007p01621

Young, R. G., and A. D. Huryn. 1998. Comment: Improvements to the diurnal upstream-downstream dissolved oxygen change technique for determining whole-stream metabolism in small streams. Can. J. Fish. Aquat. Sci. **55**: 1784–1785. doi:10.1139/f98-052

Acknowledgments

We thank two anonymous reviewers and the Associate editor whose suggestions substantially improved this manuscript. Support for this study was provided by the Virginia Coast Reserve - Long Term Ecological Research (VCR-LTER) project funded through National Science Foundation Division of Environmental Biology (DEB) grants 0080381 and 0621014, and by Chemical Oceanography (OCE) grant 0536431 to P.B., and by the Department of Environmental Sciences at the University of Virginia.

Submitted 14 August 2014
Revised 27 January 2015, 1 April 2015
Accepted 6 April 2015

Associate editor: Josef Ackerman